Variable Speed Direct Drive Induction Motors Levitated by Active Magnetic Bearings for Oil&Gas Compression Services

Lionel DURANTAY [a], Clément BIRI [a], Alain GELIN [b], Alexandre KRAL [c]

a General Electric Power Conversion, 442 Rue de la Rompure, 54250 Champigneulles, France, lionel.durantay@ge.com

b TotalEnergies, Avenue Larribau, 64018 Pau, France

c SKF S2M, 2 Rue des Champs, 27950 Saint-Marcel, France

Abstract

The purpose of this paper is to present on one hand a state of the art of innovations relating to new electrical architectures for driving high power compressors using induction motor and shaft line levitation with active magnetic bearings, and the other hand, to share return of experience on how to conduct validation tests of magnetically levitated induction rotors in high-power machines.

Keywords: *Factory Acceptance Tests, High-speed Induction Motor, Compression service, Large Magnetic bearings.*

1. Introduction about high-speed induction motors

Over the past three decades, the development of high-speed induction motors, is an alternative solution to conventional compression trains using turbines, for both onshore and offshore applications and has enabled the electrification of various compression services. The solution consists of electric motors, controlled by variable speed drive, directly driving the compressors. The entire drive train is suspended by magnetic bearings, removing the need for the oil system and associated auxiliaries. This system architecture brings with it substantial reduction in weight and footprint.

The advantages of the induction motor compared to the wound synchronous motor include no excitation system and simplified rotor construction, leading to longer run-time with fewer maintenance issues. The main components of an induction motor are (Fig. 1):

- the three-phase stator creating a rotating magnetic field, made of laminations and coils impregnated with resin with a vacuum pressure impregnation,
- the squirrel cage rotor,
- the frame supporting the stator,
- the bearings (oil lubricated or active magnetic),
- the cooling system (water cooled, or gas cooled) with axial path or bilateral paths.

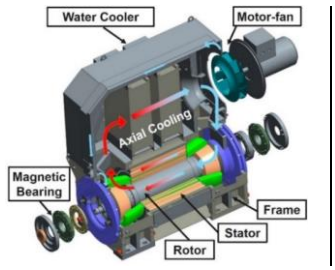

Figure 1 Induction motor design for easy maintenance.

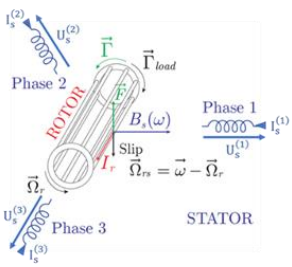

Figure 2 Torque generation with induction rotor

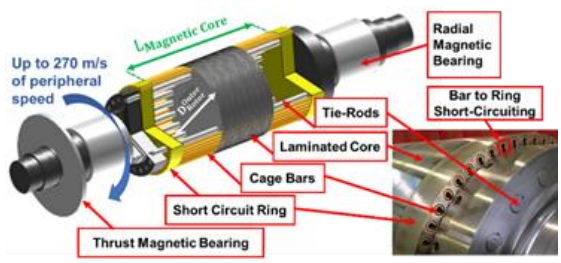

Figure 3 High-speed laminated squirrel cage rotor technology with active magnetic bearings.

The rotor consists of copper bars not insulated, short-circuited at their end by two conductive rings and constitute a "squirrel cage". The cage is swept by the rotating magnetic field. When a resistant torque $(\vec{\Gamma}_{load})$ is applied on the shaft by the load, it induces a rotor slippage (Ω_{rs}) or slip (*slip*) with a rotor pulsation (Ω) a bit lower than the stator pulsation (ω_s) which is fixed by the control of the inverter (Fig.2):

$$\Omega_{rs} = \omega_s - \Omega \quad (1)$$

$$slip = \Omega_{rs} / \omega_s \quad (2)$$

The Lorentz Force induces the rotor current (I_r) into the cage and the Laplace Force induces the torque (Γ) generation in opposite to the resistant (load) torque, where (R_{Rotor}^{Outer}) is the outer diameter of the rotor, and (K_1) and (K_2) are constant:

$$\overrightarrow{I_r} = K_1 . q . \overrightarrow{\Omega_{rs}} \wedge \overrightarrow{B_s} \quad (3)$$

$$\vec{\Gamma} = \overrightarrow{F} . R_{Rotor}^{Outer} = \left(K_2 . \overrightarrow{I_r} \wedge \overrightarrow{B_s}\right) . R_{Rotor}^{Outer} \quad (4)$$

2. High variable speed electric systems architectures

In most oil and gas use cases of electrical systems driving compressors, the standalone electric systems with gearbox are the baseline (Fig.4), combining a Direct-On-Line-fed 4-pole electric motor on oil bearings, a gearbox, and a compressor. For the TotalEnergies standpoint, this traditional architecture still presents several main concerns: large and heavy conventional system package, lubricating oil system, long commission time due to the complexity of the package, continuous gas leakage to the flare from complex dry gas seal and oil vapor from bearings (Durantay et Al., 2022). To simplify the system in terms of weight and dimension, standalone direct drive systems can be used for all compression service including gas or steam turbines replacements. The gearbox is eliminated, and the compressor is direct drive coupled to a high-speed motor. It is therefore interesting to use magnetic levitation for the whole shaft line (Fig.5). Below 30MW, standalone electric arrangements can be replaced by fully hermetic integrated moto-compressor using induction motor (Durantay et Al., 2019a) (Thibaut et Al. 2022). The process gas handled by the compressor is used to cool both the induction motor and the magnetic bearings making the unit fully hermetic, allowing to remove the gas dry seals and the conditioning system, reducing the footprint by 40% (Fig.6). Due to the large flexibility of speed range without any power derating, direct drive electric systems can be used for offshore compression services with a speed optimization to cope with the volume flow of each compressor minimizing the weight and the footprint and maximizing the efficiency of each compressor.

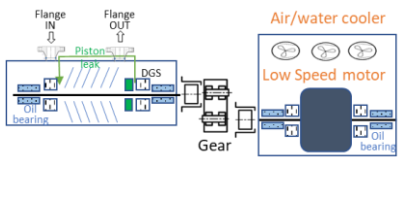

Figure 4 Oil-lubricated gearbox electric architecture.

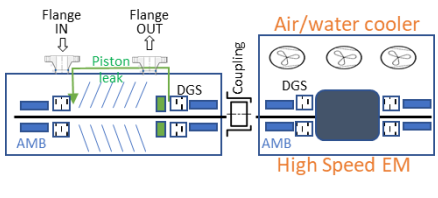

Figure 5 Standalone direct-drive electric architecture.

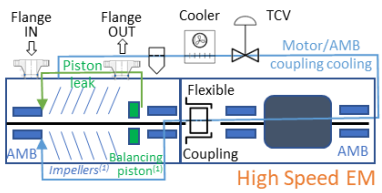

Figure 6 Integrated multi-Stage electric architecture.

An innovative technology of high-speed induction motor has been developed. The induction rotor comprises a steel lamination assembly compressed by tie rods between two end rings and two shaft ends, named shaft-less technology (Fig.3). The cage bars can expand axially through the end ring avoiding any risk of deterioration by thermal fatigue mechanism at the interface of the copper bars and the laminated shaft, respectively having coefficients of thermal expansion of $17.10^{-6}\,\mathrm{K}^{-1}$ & $12.10^{-6}\,\mathrm{K}^{-1}$. The copper bars are inserted in the slots between the two end rings to form the squirrel cage. The cage can operate reversibly up 200 °C maximizing the torque density. The laminated technology allows high efficiency in reducing the high frequencies stray load losses, and high rotor peripheral speed up to 270 m/s, providing high robustness in terms of aging and stability (Mogenier et Al., 2010) (Mogenier et Al, 2011).

Figure 7 Induction motor 16MW@9000rpm on AMBs.

Figure 8 Active magnetic bearing integration for easy maintenance.

Figure 9 Non driven end active magnetic bearing.

Figure 10 Landing bearing system.

Figure 11 Ceramic landing bearing.

As an example, TotalEnergies has decided to use this technology for an export service sized at 16MW@9000rpm (Fig.7)

which is currently the biggest reference in the word of high-speed motors levitated by active magnetic bearings (Fig.8). This high-speed direct drive system architecture using 2-pole induction motor on active magnetic bearings brings substantial reduction in weight and footprint reducing the size of the topside structure and its associated cost for a green field project. A typical cost ratio of 10 to 20 k$ per ton of installed base is the usual assumption for offshore structure (Durantay et al., 2023). As in any bearings, the AMB actuator consists of two mechanical parts, the rotor, and the stator (Fig. 9). The rotor parts are ferromagnetic laminated rings that are shrunk on the shaft. To protect the electromechanical parts in the event of bearing overload or electronic failure, auxiliary bearing set is currently used. The landing system consists of ball bearings located on the stator and having about 50 % magnetic bearing airgap against the rotor (Fig.10). Ball bearings are generally dry lubricated and are made with ceramic balls (Fig.11). The use of active magnetic bearings allows the following advantages for the electric compression: no wear, so no mechanical maintenance and unlimited lifetime, moreover no bearing noise, 200 m/s tip speed achievable, very low friction losses, no process fluid contamination by the bearing, no need for seal, oil lube system and accessories, ability to work in vacuum or hostile environments, permanent control of rotation axis, automatic balancing system because rotor spinning around its inertial axis instead of its geometrical axis, adapting static and dynamic stiffnesses for high accuracy of rotation, vibration free control, permanent monitoring of the system. The electromagnet pulling force of the active magnetic bearing (F_{pull}) is given as follow where (σ_{mag}) is the magnetic pressure and ($Area$) the airgap area:

$$F_{pull} = (\sigma_{mag}).Area = \left(B^2_{airgap} \Big/ 8\pi\ 10^{-7}\right).Area \qquad (5)$$

The magnetic induction in the airgap ($\mathrm{B_{airgap}}$) is of the order of 1.5 Tesla because of magnetic saturation in the laminations of the bearing, generating a magnetic pressure around 1 N/mm² and magnetic stiffness around 10^{-3} N/m (Fig.12). The stiffness of AMB is very soft compared to an oil film. Illustrated on a system operating at 6.9MW@13,200rpm (Fig.13), compared to oil bearings, the magnetic bearings, because of their low stiffness control (Fig.10), avoid any modes in the operating speed range of the system (Durantay et al., 2018). The rotor of the high-speed induction motor can operate in subcritical free-free mode when using magnetic bearings, meaning that the first bending mode is above operating speed defining the rotor length (Fig.14). The mode separation margin complies with API 541 even though this standard does not apply to magnetic bearings. The {Power versus Speed} capacity curves of the air-cooled induction motors at 1 and 5 bars cover most of the existing fleet of steam or gas turbines used in mechanical drive in the world (Fig. 15). Currently with existing power amplifiers generating 4 kW and up to 6 kW in peak transient conditions, it is possible to levitate rotors in rigid mode up to 10 tons spinning up to 7000 rpm. By scaling up the power of the existing technology of active magnetic bearing, it will be possible to levitate rotors up to weights of 100 tons with specific arrangements of axial thrust magnetic bearings.

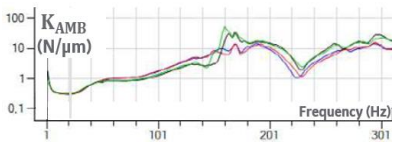

Figure 12 Active magnetic stiffness vs frequency.

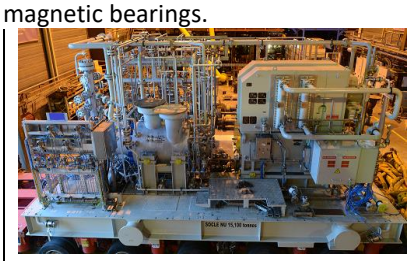

Figure 13 6.9MW-13200rpm off-shore export compression Service.

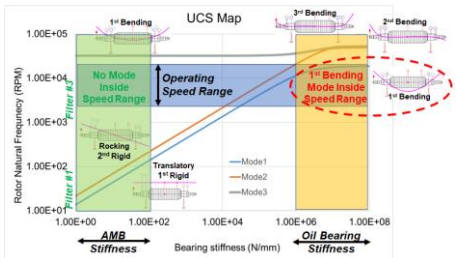

Figure 14 Undamped critical speed map 6.9MW-13,200rpm motor

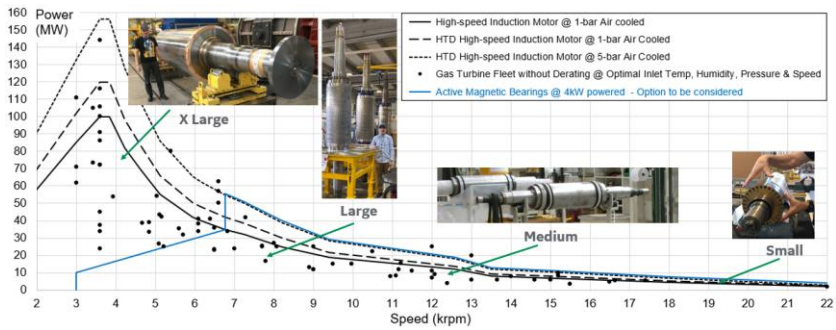

Figure 15 {Power vs Speed} capacity curve of laminated high-speed squirrel cage induction motors.

3. Factory acceptance tests of large high-speed induction motor levitated by active magnetic bearings

3.1. High-speed tests description

High power electric motors, of the order of several megawatts require factory acceptance tests. After an overspeed test useful for relieving the stresses inside the rotor, a rotor heating test is necessary for a high-speed rotor levitated by active magnetic bearings, relieving all residual stresses, reaching stable vibrations over the time in cold and hot conditions, checks residual unbalance, centrifugal and thermal expansion of the different components especially at the interface of the copper bars and the ferromagnetic laminated shaft. The principle of the test is to generate the same joule losses in the squirrel cage as in full load condition and rated speed (Ω), by adjusting the slippage (Ω_{rs}) with the drive feeding the stator at low voltage condition (Durantay et Al, 2019b) (Fig.16) (Fig.17). In this case, the slippage is:

$$\Omega_{rs} = \pm\omega_s - \Omega \tag{6}$$

When the sign of the stator pulsation is identical to the rotor speed, the machine operates in forward rotation mode and counter-rotation mode if the sign is opposite. The cage temperature rise (ΔT_{Cage}) is defined in the following heat transfer equation:

$$\Delta T_{Cage} = R_{thermal}^{rotor} . \frac{3.R_{electrical}^{rotor} . I_r^2}{Area_{cage}} \tag{7}$$

where ($R_{thermal}^{rotor}$) is the rotor thermal conductivity, ($R_{electrical}^{rotor}$) the squirrel cage electrical resistance and ($Area_{cage}$) the squirrel cage surface.

Thus, the cage temperature is adjusted with the stator voltage and frequency at rated speed condition imposed by the pony motor (see Fig.5):

$$\Delta T_{Cage} = R_{thermal}^{rotor} . \frac{slip.P}{Area_{cage}} = f(slip, U_{stator}, \omega_S) \tag{8}$$

where (P) is the absorbed power and (U_{stator}) the stator voltage.

The campaign of tests is achieved by load tests at variable power and speed conditions:

- in back-to-back arrangement without gearbox, the tested machine in motor mode and one machine in generator mode loading the system (Fig.18) (Fig.19),
- the tested machine in motor mode loaded by a slow speed generator through an intermediate gearbox.

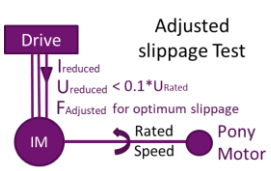

Figure 16 Rotor heating test configuration.

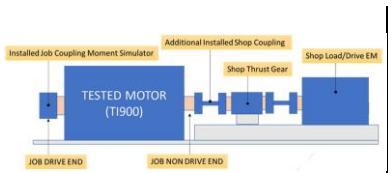

Figure 17 Direct drive coupling arrangement.

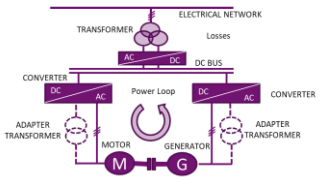

Figure 18 Back-to-back test configuration.

Figure 19 Back-to-back test arrangement.

3.2. High-speed test without axial thrust

The test described is a load test with a gearbox. The high-speed motor tested is an induction motor levitated by active magnetic bearings operating at a nominal speed of 13,840 rpm. The motor is connected to the gearbox with a flexible coupling (Fig.20). The load generator, operating at low speed, is coupled on the other side of the gearbox. This test configuration is conventional. During the increase in speed at no load condition, significant vibrations and shaft displacements are respectively measured on the casing of the gearbox and on the high-speed rotor.

Analysis of vibration signals demonstrates the following cause -effect mechanism. A measurement of the axial displacement of the shaft line highlights an axial resonance at approximately 5Hz self-excited by the slippage modulation of the rotor magnetic field inducing amplitudes of the order of millimeters (Fig.22) and axial vibrations of the gearbox casing (Fig.21) of the order of 9 mm/s rms at 13,000 rpm (Fig.23). This induces a doubling of the amplitude of the high-speed rotor shaft displacements with around 20 umpp of unbalance at 1X the speed of rotation and 20 umpp at 5 Hz (Fig.24). Motor-compressor architectures incorporate the thrust bearing on the compressor side. The electric motors tested do not have an axial thrust bearing. This is not a problem when testing a conventional low-speed oil-bearing motor, but it becomes an issue for high-speed motors levitated by AMB. The problem is solved by inserting between the high-speed coupling and the gearbox a mechanical thrust.

Figure 20 Load test with gearbox (high-speed motor on the right)

Figure 21 Velocimeters instrumentation on gearbox.

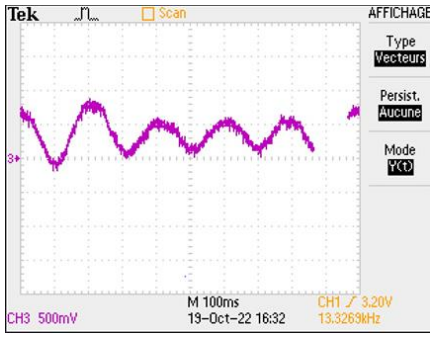

Figure 22 Axial displacement of the induction rotor.

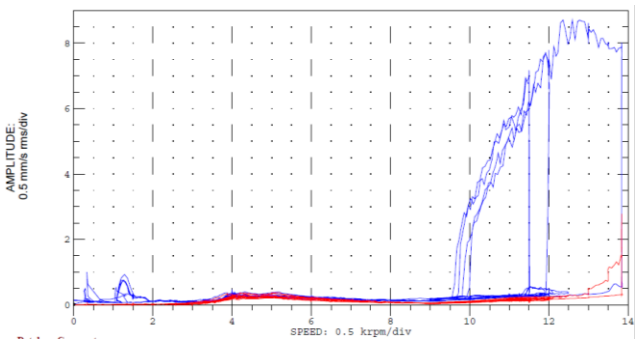

Figure 23 Gearbox Axial vibration @ 13,840rpm.

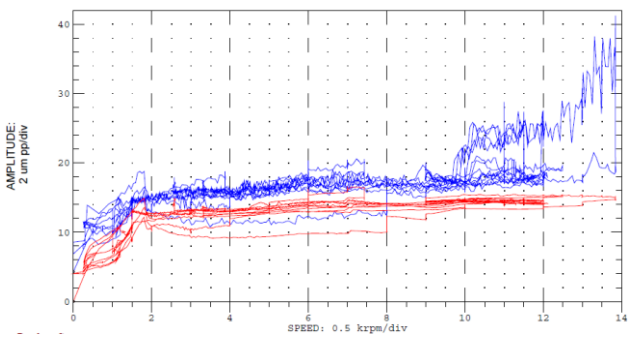

Figure 24 Induction rotor shaft displacements @ 13,840rpm.

3.3. High-speed test with axial thrust

The recommended test setup is to use an axial thrust bearing equipped with ball bearing lubricated by an oil mist. For the rotor heating tests or partial load tests, a high-speed induction motor is used to drive the main motor to be tested. This motor can deliver a power of 6 MW at 15,000 rpm (Fig.25) (Fig.26). It is equipped with customized active magnetic bearings (Fig.27) (Fig.28). This testbench motor has been used since 2012 for high-speed testing.

Tests of the 16MW@9000rpm motor are carried out with this axial thrust bearing (Fig.29) (Fig.30). Vibrations at 8,940 rpm, at no load and at full load at 16 MW are less than 50 umpp (Fig.31) with an alarm and trigger threshold set by mutual agreement with the end user at 100 umpp and 150 umpp.

Figure 25 Testbench motor on AMB (on left) with thrust bearing gear (on right).

Figure 26 Testbench motor magnetic bearing integration.

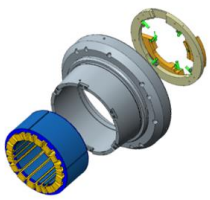

Figure 27 Testbench motor active magnetic bearing.

Figure 28 Testbench motor active magnetic bearing actuator.

Figure 29 Rotor heat test arrangement (Testbench motor side).

Figure 30 Rotor heat test arrangement (16MW Motor side).

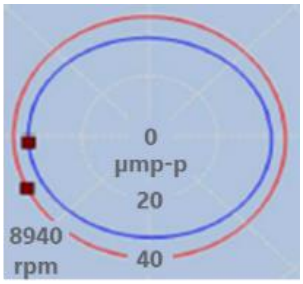

Figure 31 16MW rotor shaft displacement @ 8,940rpm.

4. Conclusion

This publication describes the state of the art in electric compressor drive architectures, in particular the high-speed induction motor technology which makes it possible to cover almost all the demands of compression services in the Oil & Gas market up to 100MW, including gas and steam turbines replacements. Associated with this motor technology, the magnetic bearings allow great flexibility of use for wide ranges of speeds by eliminating the use of oil, with limited risks of interaction with the foundation, and integrated moto-compressor system cooled by the process gas. Unlike a gas turbine or a steam turbine which respectively produce an average of 5,000 tons and 10,000 tons of greenhouse gas per year, the high-speed induction motor produces no polluting emissions if it is powered by carbon-free electricity from a nuclear power plant or a renewable energy source such as offshore wind turbines using direct drive permanent magnet generators (Fig.32 & 33). For these large electrical motors levitated by active magnetic bearings, the recommended test setup is to use an axial thrust bearing equipped with ball bearing lubricated by an oil mist, to reduce the risk of vibrational interactions between the motor to be tested and the testbench machine.

Figure 32 6MW offshore windmill field

Figure 33 6MW@11rpm PM generator

References

API Standard 541:Fifth Edition (2014) Form-wound Squirrel Cage Induction Motors—375 kW (500 Horsepower) and Larger.

Durantay L, Alban T, Siala S and Billaud A (2018) Selection and Tests of Innovative Variable-Speed Motor-Compressor Solutions for a 55-MW Full Electric Offshore Platform Maximizing Availability and Efficiency With Better Environmental Impact. IEEE Transactions on Industry Applications, 55(6).

Durantay L, Gelin A, Thibaut E and Vidalenc Y (2019a) Integrated Motor Compressor versus Conventional Solution. In 16th PCIC Europe Conference, Paris, FR, 7-9 May 2019.

Durantay L, Clark T, Roth L and Galmiche C (2019b) Alternative Package of Tests to Reduce Capex and Delivery Time of Large LNG Train Using Induction Machine Fed by VSI Drive Technology up to 120MW. In 66th IEEE IAS PCIC technical Conference, Vancouver, CA, 8-12 Sep 2019.

Durantay L, Gamiche C, Grosselin C and Verdot P (2022) Innovative Variable Speed Systems Using Induction Motor for Gas Compression. In 8th IEEE-PCIC Middle East Conference, Al Khobar, KSA, 15-16 November 2022.

Durantay L, Gelin A, Thibaut E and Roth L (2023) Rex and Recommandations for Mechanical Integration of Large High-speed Motors. In 19th PCIC Europe Conference, Milano, IT, 6-8 June 2023.

Mogenier G, Dufour R, Ferraris-Besso G, Durantay L and Barras N (2010) Identification of Lamination Stack Properties: Applications to High-speed Induction Motors. IEEE Transactions on Industrial Electronics, 57(1).

Mogenier G, Baranger T, Dufour R, Durantay L and Barras N (2011) Efficient Model Development for an Assembled Rotor of an Induction Motor Using a Condensed Modal Functional. Journal of Computational and Nonlinear Dynamics, 6(2), April, pp. 1–8.

Thibaut E, Pellerin O, Durantay L, Bouyssou S, Bouteille A and Garaudee L (2022) Selection and Return of Experience of Integrated Moto-compressors on Two Oil&Gas Sites. In 18th PCIC Europe Conference, London, UK, 6-8 June 2022.